JCTC Journal of Chemical Theory and Computation

Article

pubs.acs.org/JCTC

Toward Molecular-Level Characterization of Photoinduced Decarboxylation of the Green Fluorescent Protein: Accessibility of the Charge-Transfer States

Bella L. Grigorenko,[†] Alexander V. Nemukhin,*[,†,‡] Dmitry I. Morozov,[†] Igor V. Polyakov,[†] Ksenia B. Bravaya,[§] and Anna I. Krylov[§]

[†]Department of Chemistry, M.V. Lomonosov Moscow State University, Moscow 119991, Russia

[‡]Institute of Biochemical Physics, Russian Academy of Sciences, Moscow 119334, Russia

[§]Department of Chemistry, University of Southern California, Los Angeles, California 90089-0482, United States

Supporting Information

ABSTRACT: Irradiation of the green fluorescent protein (GFP) by intense violet or UV light leads to decarboxylation of the Glu222 side chain in the vicinity of the chromophore (Chro). This phenomenon is utilized in optical highlighters, such as photoactivatable GFP (PA-GFP). Using state-of-the-art quantum chemical calculations, we investigate the feasibility of the mechanism proposed in the experimental studies [van Thor et al. *Nature Struct. Biol.* **2002**, *9*, 37−41; Bell et al. *J. Am. Chem. Soc.* **2003**, *125*, 37−41]. It was hypothesized that a primary event of this photoconversion involves population of a charge-transfer (CT) state via either the first excited state S_1 when using longer wavelength (404 and 476 nm) or a higher excited state when using higher energy radiation (254 and 280 nm). Based on the results of electronic structure calculations, we identify these critical CT states (produced by electron transfer from Glu to electronically excited Chro) and show that they are accessible via different routes, i.e., either directly, by one-photon absorption, or through a two-step excitation via S_1. The calculations are performed for model systems representing the chromophore and the key nearby residues using two complementary approaches: (i) the multiconfigurational quasidegenerate perturbation theory of second order with the occupation restricted multiple active space scheme for configuration selection in the multiconfigurational self-consistent field reference; and (ii) the single-reference configuration interaction singles method with perturbative doubles that does not involve active space selection. We examined electronic transitions with nonzero oscillator strengths in the UV and visible range between the electronic states involving the Chro and Glu residues. Both methods predict the existence of CT states with nonzero oscillator strength in the UV range and a local excited state of the chromophore accessible via S_1 that may lead to the target CT state. The results suggest several possible scenarios for the primary photoconversion event. We also demonstrate that the point mutation Thr203His exploited in PA-GFP results in shifting the light wavelength to access the CT up to 20 nm, which suggests a possibility of a rational design of photoactivatable proteins in silico.

INTRODUCTION

Fluorescent proteins (FPs) from the family of the green fluorescent protein (GFP) attract considerable attention owing to their use as genetically encoded fluorescent probes for in vivo imaging.[1−8] The FPs whose optical properties can be modified by light, i.e., the so-called photoactivatable (PA) and photoswitchable (PS) FPs, further extend the scope of bioimaging applications. For example, they can be used as optical highlighters, fluorescent timers as well as in super-resolution microscopies.[9−15] The mechanistic details of these phenomena are not yet fully understood. The structural motifs appear to be rather diverse, for example, changes in absorption wavelength in PA-GFP (and PS-GFP2) are due to decarboxylation of a nearby residue, whereas green-to-red conversion of several FPs (Kaede, KirkGR, Dendra2, and Eos) and orange-to-far-red conversion (PSmOrange) is attributed to the extension of the chromophore's π-system. Other examples include cis−trans isomerization of the chromophore (Dronpa, KFP1, and mTFP0.7), sometimes in conjunction with the π-system extension (PAmCherry and PATagRFP). The structural basis of some photoconversions, such as oxidative and anaerobic redding,[12] is still unknown.

The focus of this work is on one of the first-characterized photoconversions, the conversion of GFP from the blue to green absorbing form upon intense UV or visible light exposure.[16,17] Van Thor and co-workers have observed an irreversible change in the absorption spectra of the wt-GFP upon exposure to intense 3.07 eV (404 nm, visible) or 4.88 eV (254 nm, UV) light.[16] Whereas the wt-GFP has two pronounced peaks at 3.12 and 2.59 eV (398 and 478 nm, respectively), the irradiated protein features a single absorption peak at 2.57 eV (483 nm). The reduction in mass of 44 Da was observed in mass spectrometry studies of the photoproduct, which therefore was called GFP_{483}. The crystal structure of GFP_{483} determined with 1.8 Å resolution (Protein Data Bank (PDB) code: 1HCJ)[16a] has identified the difference between wt-GFP and GFP_{483} as a change in the local structure near the Glu222 position—apparently, a decarboxylation reaction (loss

Received: January 24, 2012

   dx.doi.org/10.1021/ct300043e | *J. Chem. Theory Comput.* XXXX, XXX, XXX−XXX

of CO_2) of this amino acid side chain took place. The authors reported that the phototransformation obeys first-order kinetics with a small activation barrier (~0.24 kcal/mol) derived from temperature dependence of the rate. The quantum yield at 254 nm was 0.03, and the authors noted distinctly lower quantum yield at lower energies. Based on the analogy with organic photochemistry, they posited that the electronically excited chromophore accepts an electron from Glu222, which initiates a Kolbe-type rearrangement.

The subsequent study by Bell et al.[17] has demonstrated that the rate of the light-induced decarboxylation of wt-GFP strongly depends on the excitation wavelength and decreases at lower energies (i.e., 254 > 280 > 476) by more than 2 orders of magnitude. They also noted that photoconversion at 404 and 476 nm did not occur below a certain laser power threshold. For example, no photoconversion occurred upon irradiation of the sample by 404 nm light at 6 mW/cm^2 even after 6 h of irradiation. This threshold behavior is strongly suggestive of a two-photon process; however, the reported linear dependence on laser power between 50 to 1 mW/cm^2 did not support this hypothesis.[17] The authors have noted difficulties in quantifying the lower energy photoconversion due to production of reactive oxygen species leading to photobleaching. The authors proposed that higher and lower energy photoinduced decarboxylation proceeds via different electronic states, i.e., via either the lowest excited state (S_1) of the chromophore (Chro) in a lower energy regime (2.61 or 3.07 eV/476 or 404 nm) or a higher excited state when using 4.88 eV (254 nm) light. A more recent study[16b] has discussed the initial steps of electron-transfer process in terms of Marcus theory and free-energy differences between the charge-transfer (CT) states; however, the analysis was limited by the lack of quantitative information about energy differences between the states involved. Notably, a possibility of a direct excitation to the CT states has not been considered. Later, the power dependence of the decarboxylation reaction in the Thr203Val mutant has been investigated by using a more sensitive technique, accumulative femtosecond spectroscopy.[18] This study has found that using 400 nm (3.1 eV) excitation, the decarboxylation requires two photons, whereas at lower excitation energies (800 nm, 1.55 eV), it becomes a three-photon process. The authors[18] have concluded that it is a higher excited state of the neutral chromophore that needs to be excited to facilitate photoconversion; however, no information about the character of this state has been offered.

As mentioned above, the decarboxylation phenomenon is utilized in optical highlighters, such as photoactivatable GFP (PA-GFP). As such, Patterson and Lippincott-Schwartz[19] developed a new GFP mutant (Thr203His) with an improved optical contrast achieved by reducing the minor peak absorbance relative to wt-GFP. Recently, the crystal structures of PA-GFP in the initial and activated (decarboxylated) states have been reported (PDB codes: 3GJ1, 3GJ2).[20]

The identification of the primary event in photoinduced decarboxylation by using molecular modeling tools is important as it may suggest a way to improve properties of photoactivatable FPs. For example, by changing relative energies of the states involved, one may be able to reduce undesirable readout activation. Detailed characterization of electronic states of GFP (with the chromophore in the neutral form) by quantum chemistry methods is the first step toward mechanistic understanding of photoactivation. It should be noted that this system presents a challenging case for the electronic structure theory. First, unlike the anionic species, the excited states of the neutral (protonated at the phenolic oxygen) form of the chromophores from the GFP family are difficult to describe even in the gas phase[21−29] because of strong mixing of electronic configurations in the excited-state manifold, which calls for high-level electronic structure methods. An adequate representation of the chromophore's environment is also difficult. Several papers[21,23,25,28−31] have analyzed the effect of the nearby residues as well as the entire protein and solvent on different properties including excitation and ionization energies. For the anionic chromophores, most of the studies agree that the lowest excitation energy is not much affected by the protein environment, which can be explained by the small change of the dipole moment upon excitation.[28,30,31]

The situation appears to be very different for the neutral chromophore. The study of Laino et al.[21] has shown that hydrogen bonding between the chromophore and the side chains of Arg96 and Gln94 and even water molecules leads to a noticeable red shift (0.3−0.4 eV, more than 30 nm) of the S_0−S_1 excitation energy. Later, Hasegawa et al.[23] have calculated a manifold of excited states for model systems consisting of the bare neutral GFP chromophore (model I), the chromophore in the field of point charges representing the rest of protein (model II), and a molecular cluster composed of Chro, the side chains of Ser205, Glu222, and a water molecule in the field of point charges (model III). The authors used the B3LYP/6-31G* optimized geometry and the symmetry-adapted cluster configuration interaction (SAC-CI) method to compute excited-state energies. They reported S_0−S_1 excitation energies (3.23, 3.21, and 3.27 eV for models I, II, and III, respectively) that were amazingly close to the experimental absorption maximum of wt-GFP (3.12 eV or ~400 nm). In particular, their results suggested an almost negligible effect of the protein, although the data for the molecular cluster from model III without point charges were not reported (thus, it is not possible to assess the effect of the protein beyond the nearby residues). Based on the analysis of the molecular orbitals and the configuration interaction expansion coefficients, the authors assigned the fifth singlet state in model III as a CT state corresponding to the electron transfer from Glu222 to Chro. According to Figure 3 from ref 23 such electron transfer is associated with the transition from an orbital spanning Glu222 and Chro to the π^*-orbital of Chro. The corresponding excitation energy was reported to be 4.18 eV (296 nm), and the oscillator strength was reported as 0.027 au. The authors hypothesized about a possible role of this excited state (from the model III calculations) in the photoinduced decarboxylation of GFP.

The recent theoretical paper[29] focused on quantum chemical simulations of the S_0−S_1 absorption band of wt-GFP with the anionic and neutral chromophores when applied complete active space self-consistent field (CASSCF) based multiconfigurational perturbation theory (CASPT2), time-dependent density functional theory (TDDFT), and quantum Monte Carlo (QMC) methods within a quantum mechanics/molecular mechanics (QM/MM) scheme. For the neutral GFP chromophore, the authors reported a widespread of values for the vertical excitation energy in the gas phase and in the protein environment.[29] The CASPT2 values varied from 3.15 to 3.85 eV depending on the treatment of perturbation corrections even when the exactly the same (and quite large) active space was employed in underlying CASSCF. In accord with the previous studies,[25,26] the authors noted difficulties in

performing the CASSCF calculations for the neutral models because the bright state does not appear as the second CASSCF root. Contrary to the gas-phase chromophore case, the CASPT2 results for the protein model are amazingly stable for the active spaces larger than (10/10) varying between 3.53 and 3.56 eV.[29] The reported best estimate of the S_0-S_1 excitation energy for the model protein, 3.53 eV (370 nm), is about 30 nm (0.4 eV) apart from the experimental value.[1,32] No results for the higher excited states were reported in ref 29.

The goal of the present work is two-fold: First, we characterize electronically excited states of the model system representing the neutral GFP chromophore in the binding pocket of the protein by using state-of-the-art quantum chemistry methods. The calculations allowed us to identify states that have Glu222 → Chro CT character and to determine whether such states have sufficient oscillator strength and excitation energies to be accessible by the UV or visible light, either directly or in a two-step process. Second, we test whether the point mutation Thr203His in GFP affects energies of higher excited states that are likely to be involved in the photoinduced decarboxylation of PA-GFP. If a noticeable shift of CT states can be induced by mutations, theoretical modeling may be employed for rational design of photoactivatable proteins in silico. For example, mutations reducing read-out activation may be designed.

COMPUTATIONAL DETAILS

Characterization of the excited states, and especially CT states, requires careful selection of the model system. The residues forming the hydrogen-bond network connecting Chro and Glu222 as well as nearby charged groups that may affect the energy of the CT states should be included in the QM part. Our model system was constructed as follows: The initial coordinates of heavy atoms were taken from the crystal structure of wt-GFP with the PDB code 1EMA.[33] After addition of hydrogen atoms, the entire protein structure was optimized by QM/MM calculations with the effective fragment potential (EFP) description of the MM part. We employed the flexible effective fragment version[34,35] of the QM/EFP method.[36] The QM part included the following moieties: the chromophore, the side chains of Arg96, Ser205, and Glu222, and the water molecule connecting Ser205 and the oxygen atom of the chromophore by hydrogen bonds. For the purpose of the present study, we focus on the neutral (protonated at the phenolic oxygen) form of Chro and negatively charged Glu222. Density functional theory with the PBE0 functional and the cc-pVDZ basis set was used to calculate energies and forces in the QM part. The MM part was represented by a collection of flexible effective fragments, with the interactions between the MM fragments described by the AMBER force field. The computed structure was verified by superimposing it onto the available crystal structures with the PDB codes 1EMA[33] and 1GFL.[37] We carefully examined the hydrogen-bond network in the chromophore vicinity to ensure that the calculated geometry adequately reproduces the protein structure in the chromophore's binding pocket. Supporting Information includes additional details on the QM/MM model as well as the optimized coordinates of the QM subsystem (Table S1, Supporting Information).

Next, we selected a smaller molecular cluster from the above QM/MM model to be used as the QM part in excited-state calculations. The structure of this cluster is shown in Figure 1. The effect of the rest of the protein was described either by representing the MM part by effective fragments[34,35] or by the force field (AMBER) point charges of the MM atoms.

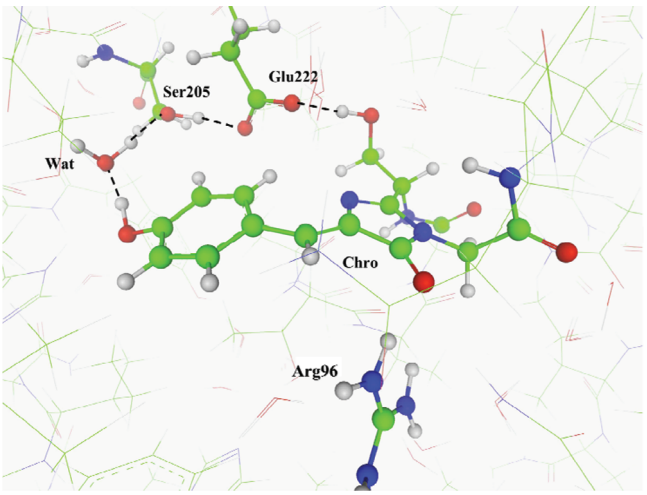

Figure 1. The model cluster (balls and sticks) mimicking the protein-bound chromophore and the nearby residues that were used for calculations of excited-state energies and oscillator strengths.

The point mutation Thr203His was simulated by modifying the system modeling wt-GFP (with Thr at position 203) as described above. We manually replaced Thr by His following motifs of the crystal structure 3GJ1[20] and partly reoptimized coordinates in the QM/MM(EFP/AMBER) approach keeping the residue at position 203 in the MM subsystem as before.

The excited states in these model systems were characterized by several quantum chemical approaches. Two variants of multiconfigurational SCF (MCSCF) methods were used, the complete active space (CASSCF) with the state-averaging (sa) procedure, and the occupation restricted multiple active space (ORMAS)[38] algorithm. Dynamical correlation was described by multiconfigurational quasidegenerate perturbation theory of the second order (MCQPDT2)[39] and the extended version of MCQDPT2, XMCQDPT2.[40] All MCSCF-based calculations were performed using the GAMESS(US)[41] and Firefly[42] packages, which is partially based on the GAMESS(US) code. Selections of the orbital active space and configurations for each calculation are described below.

Most of the MCSCF calculations reported below were performed using the sa(M)-CASSCF(12/11) protocol, i.e., with 12 electrons distributed over 11 active orbitals and averaging over the first M roots in CASSCF. Based on the preliminary inspection of the wave function coefficients as well as the results of previous studies of the isolated neutral chromophore,[24−26] we concluded that at least three lowest roots ($M = 3$) should be included in state averaging. In order to describe the Glu222 → Chro CT states by MCSCF-based methods, the orbital active space should include both the Chro and Glu orbitals, which leads to a prohibitively large CAS expansion. To overcome this problem, we employed the ORMAS algorithm[42] within the MCSCF procedure. By dividing the total orbital space into multiple subspaces and specifying different occupation values for each subspace, ORMAS allows reduction of the number of configurations in MCSCF expansions.

As an alternative approach that does not require active space selection, we employed the scaled opposite-spin configuration

dx.doi.org/10.1021/ct300043e | J. Chem. Theory Comput. XXXX, XXX, XXX−XXX

Table 1. Vertical S_0-S_1 Excitation Energies (eV) for Model Systems with the Neutral Form of the GFP Chromophore Computed by Different Methods[a]

model system	computational protocol	excitation energy, eV	reference
QM cluster (Chro, Ser205, Glu222, Arg96, Wat; Figure 1)	XMCQDPT2/sa-CASSCF(12/11)/cc-pVDZ	3.08	this work
QM cluster (Chro, Ser205, Glu222, Arg96, Wat; Figure 1) + effective fragments for the rest of the protein	XMCQDPT2/sa-CASSCF(12/11)/cc-pVDZ	3.40	this work
QM cluster (Chro, Ser205, Glu222, Arg96, Wat; Figure 1)	SOS-CIS(D)/cc-pVDZ	3.23	this work
QM cluster (Chro, Ser205, Glu222, Arg96, Wat; Figure 1) + point charges for the rest of the protein	SOS-CIS(D)/cc-pVDZ	3.78	this work
QM cluster (Chro, Arg96, Gln94, 2 Wat)	CAS(6/6)-CI/MNDO	3.10	ref 21
QM cluster (Chro, Ser205, Glu222, Wat) + point charges for the rest of the protein	SAC−CI/DZP	3.27	ref 23
QM cluster (Chro, Ser205, Glu222, Thr203, Thr62, Arg96, His148, 2 Wat)	ZINDO	3.01	ref 25
Cromophore + point charges for the rest of the protein	CASPT2/CASSCF(16/14)/ANO-S-PVDZ	3.53	ref 29
	TDDFT(different functionals)/aug-cc-pVDZ	3.07−3.61	

[a]The experimental absorption maximum of wt-GFP is 3.12 eV at room temperature[1] and 3.05 eV at low temperature.[32]

interaction method SOS-CIS(D).[43,44] CIS(D) is a single-reference method, which can be described as an approximation to equation-of-motion coupled cluster with single and double excitations (EOM-CCSD).[45] Scaled opposite-spin correction improves CIS(D) accuracy and, along with density fitting, results in a reduced scaling (N^4). SOS-CIS(D) has been shown to yield accurate results for similar chromophores[46,47] and is capable of describing both locally excited and CT states. However, it may break for states with doubly excited character or when excited states are degenerate at the CIS level. SOS-CIS(D) calculations were performed with the Q-Chem program.[48]

We use the following notations throughout the paper: symbols S_n denote singlet excited states localized on the chromophore moiety, whereas S_{CTn} refer to the singlet CT states of the Glu → Chro character. In the SOS-CIS(D) calculations, both types of states (S_n and S_{CTn}) appear in a singe calculation; however, in MCSCF-based calculations they are computed using separate MCSCF setups.

RESULTS

S_0-S_1 Excitation Energy in wt-GFP. We begin by assessing the accuracy of the computational protocols employed for the systems mimicking wt-GFP with both types of the chromophore, anionic and neutral. As the results below demonstrate, the calculations performed at the highest level of theory are sufficiently accurate to be directly compared to the relevant experimental data.

To build a model system with the anionic protein-bound chromophore (described also in ref 31), the hydrogen-bond network (dashed lines in Figure 1) was rearranged by shifting the protons from Chro to Glu222. Following QM/MM geometry optimization, the vertical S_0-S_1 excitation energy computed at the XMCQDPT2/CASSCF(12/11)/cc-pVDZ level of theory was found to be 2.69 eV (or 460 nm). This value is within 0.1 eV from the experimental absorption band maximum of wt-GFP, 2.59 eV (478 nm) at room temperature,[1] or 2.63 eV (471 nm) at low temperature.[32] The ability of SOS-CIS(D) to accurately describe properties of GFP with the anionic chromophore was assessed in ref 31.

Next, we turn to the more challenging case of the neutral chromophore. Table 1 collects the results of the present and previous calculations of the vertical excitation energy of the bright state for model systems mimicking wt-GFP with the protonated (neutral) form of the chromophore.

To avoid overcrowding of Table 1, we selected the representative values from the present and previous[21,23,25,29] studies. We keep in mind that the results are fairly sensitive to such details as a choice of the QM cluster, the method used to optimize ground-state geometry, selection of the acive space, the number of roots in CASSCF state-averaging, and so forth, as partly illustrated by our data included in Table S2, Supporting Information. The conclusions below are formulated taking into accout the entire scope of results for the model systems with the neutral chromophore.

First, we observe that the effect of the protein beyond the nearby residues (e.g., our QM cluster) is quite substantial (0.3−0.5 eV). Such effect on the S_0-S_1 excitation energy is small only when using the bare neutral chromophore as a quantum subsystem in the field of effective fragments representing the rest of the protein. As shown in Table S2, Supporting Information, we could reproduce the observation of Hasegawa et al.[23] by using the CASSCF(12/11) calculations: For the neutral chromophore only in the QM part, we obtained S_0-S_1 excitation at 5.32 eV without EFPs and 5.23 eV with EFPs. However, extension of the QM subsystem by including the nearby molecular groups (Arg, Glu, Ser, water), which leads to the QM cluster shown in balls and sticks in Figure 1, considerably down-shifts the S_0-S_1 energy gap. This result is in qualitative agreement with the conclusions of Laino et al.[21] Addition of the electrostatic field of the rest of protein through effective fragments up-shifts the excitation energy. We conclude that the presence of molecular groups in the vicinity of Chro, the most influential of which is the charged side chain of Arg96, is responsible for a noticeable red shift of the excitation energies of bare Chro, while the effect of the rest of protein (described by either EFs or point charges) serves to up-shift the values for the QM cluster. Overall, we expect that the excitation energies for the QM cluster (Figure 1) are underestimated due to the neglect of the rest of the protein.

Clearly, apart from the semiempirical (ZINDO, MNDO) values,[21,25] the results in Table 1 converge to 3.4 eV, which is 0.3 eV higher that the experimental value.[1,31] Our best value, 3.40 eV, is obtained for the cluster (Chro, Ser205, Glu222, Arg96, Wat; Figure 1) in the field of effective fragments by using XMCQDPT2/sa(3)-CASSCF(12/11)/cc-pVDZ. The use of the active space corresponding to distribution of 12

dx.doi.org/10.1021/ct300043e | J. Chem. Theory Comput. XXXX, XXX, XXX−XXX

electrons over 11 orbitals is, of course, a compromise, since the CASSCF-based treatment of all π-electrons of the chromophore in our QM/MM calculations is too expensive. Further increase of the active space may lower the excitation energy, which would bring it to a better agreement with the experiment.

Although such a computationally demanding approach is highly desirable for obtaining accurate results, it cannot be applied for calculations of highly excited states, which are the primary target of this work. As discussed below, up to eight singlet states of the model system corresponding to the local chromophore excitations should be considered to interpret the decarboxylation experiments in a lower excitation energy regime of 3.07 eV (404 nm).[16] Consequently, we adopted a less ambitious computational protocol. Since the neighboring groups are mandatory for characterization of the CT states, we consider the QM cluster (Chro, Ser205, Glu222, Arg96, Wat) shown in balls and sticks in Figure 1 as the smallest adequate model. The analysis of the data in Table 1 suggests that the calculations for such model system with either XMCQDPT2/sa-CASSCF(12/11)/cc-pVDZ or SOS-CIS(D)/cc-pVDZ should provide good estimates for the local excitation energies of the chromophore in GFP, in virtue of error cancellation. That is, although these approaches overestimate excitation energies due to their shortcomings (incomplete active space in CASSCF or lack of multiconfigurational character of the reference state in CIS(D)), on the other hand, these values are underestimated due to the neglect of the rest of the protein.

S_0–S_n ($n \geq 1$) Excitations in wt-GFP with the Neutral Form of the Chromophore. Since the decarboxylation of GFP occurs upon intense irradiation by visible light at 404 nm (3.07 eV) corresponding approximately to the S_0–S_1 transition, we intend to locate a higher excited state, let us call it S_X, that may be accessible via S_1. Table 2 lists the results of the XMCQDPT2/sa(10)-CASSCF(12/11)/cc-pVDZ calculations for transitions between the singlet states of the model QM cluster (Chro, Ser205, Glu222, Arg96, Wat; Figure 1). In these computations, the first 10 states (M = 10) were included in the CASSCF state averaging. The respective S_0–S_1 excitation energy is 3.18 eV, as compared to 3.08 eV (Table 1) attainable with the minimal set of three states (M = 3) needed for a proper description of the neutral chromophore.

Table 2. Excitation Energies (eV) and Oscillator Strengths (f) for the Transitions within the Manifold of Singlet States Corresponding to the Local Excitations of Chro Computed by XMCQDPT2/sa(10)-CASSCF(12/11)/cc-pVDZ for the QM Cluster (Figure 1)[a]

state	f (S_0–S_n)	$E(S_n) - E(S_0)$, eV	f (S_1–S_n)	$E(S_n) - E(S_1)$, eV
S_1	**1.7**	**3.18**		
S_2	0.7	3.83	0.25	
S_3	0.04	4.14	0.01	
S_4	0.3	4.99	0.002	
S_5	0.07	5.01	0.05	
S_6	0.9	5.71	0.3	2.53
S_7	**0.001**	**6.18**	**0.5**	**3.00**
S_8	0.2	6.19	0.02	
S_9	0.3	6.64	0.03	

[a]In the last column we show excitation energies with non-negligible oscillator strengths.

The most important result is that it appears to be possible to populate a highly excited state S_X (S_7 at the CASSCF level of theory) via S_1: the corresponding transitions S_0–S_1 (f = 1.7) and S_1–S_X (f = 0.5) are sufficiently bright. Note that the two transition energies, 3.18 (390 nm) and 3.02 eV (411 nm) are also fairly close; therefore, we conclude that intense visible light with the wavelength around 400 nm can be used to reach S_X via S_1, either sequentially or by resonance-enhanced two-photon absorption. Thus, this could be the "doubly excited state" accessed by two-photon absorption (using 400 nm) in the ultrafast pump–probe study.[18]

The character of the S_X (S_7) state is illustrated (Figure 2) by the molecular orbitals (MOs) obtained with the averaged CASSCF densities whose occupation numbers change upon this transition. This pair of MOs can be thought of as the initial and final MOs in the transition, analogous to the highest occupied molecular orbital (HOMO) and the lowest unoccupied molecular orbital (LUMO) giving rise to the S_1 excited state.

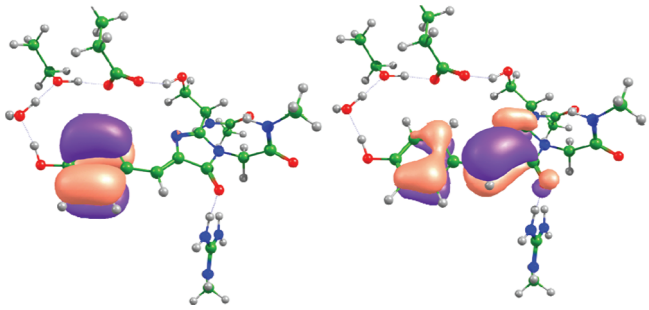

Figure 2. The initial and final MOs giving rise to the S_X excited state. Left: The MO occupied in S_0, and right: the MO occupied in S_X.

As shown in Table 3, the SOS-CIS(D)/cc-pVDZ calculations also predict an excited state around 6 eV with a noticeable oscillator strength (Table 3). At this level of theory we were able to estimate the effect of the rest of protein by point charges. As expected, a blue shift of 0.3 eV due to the electrostatic field of the protein was obtained; furthermore, two states at 6.05 and 6.25 eV with oscillator strengths 0.5 and 0.2 were found, in contrast to only one state (at 5.67 eV) in simulations without charges.

Table 3. Transition Energies (eV) Corresponding to the Local Chromophore Excitations Calculated by SOS-CIS(D)/cc-pVDZ[a]

model	S_0–S_1	S_0–S_x
QM cluster (Figure 1)	3.23 (1.3)	5.67 (0.2)
QM cluster (Figure 1) + point charges	3.78 (1.2)	6.05 (0.5) 6.25 (0.2)

[a]Oscillator strengths are given in parentheses.

In summary, by using two different quantum chemistry approaches, MCSCF-based and SOS-CIS(D), we identified a locally excited state S_X at about 6 eV that can be accessed via S_1.

Excitations to the CT States S_{CT}. Using standard CASSCF-based procedures to calculate excited states corresponding to electron transfer from the Glu orbitals to the orbitals localized on Chro is prohibitively expensive because of a huge size of active space comprised of occupied and virtual orbitals of the two moieties, Glu and Chro. To circumvent this problem, we employed the ORMAS scheme[42] in which the

dx.doi.org/10.1021/ct300043e | J. Chem. Theory Comput. XXXX, XXX, XXX–XXX

MSCSF expansion is produced by taking products of separate full CI expansions generated within each orbital subspace. To this goal, we extended the CASSCF(12/11) active space by adding three occupied orbitals localized on Glu. The total active space in MCSCF/ORMAS calculations consisted of 18 electrons in 14 orbitals, which was broken into the three following subspaces: (i) 3 Glu orbitals; (ii) 6 occupied Chro orbitals; and (iii) 5 virtual orbitals; and the electron transitions were allowed only from the first to the third subspace. Doubly occupied orbitals from the subspace (ii) could not be excluded from the active space and placed among inactive orbitals since the MCSCF orbital optimization procedure would return them to the active space instead of Glu orbitals. Restrictions on interspace orbital rotations imposed by ORMAS allowed us to keep the Glu orbitals in the active space. As in the case of local excited states, the state averaging procedure should be applied. We included five lowest roots in state-averaging, more than actually is required, since we did not know in advance which particular CT states are accessible from S_0.

With such partitioning of the orbital space, the Glu → Chro singlet CT states, S_{CTn}, appeared as the CI roots immediately following the ground state, since excitations from the six occupied chromophore orbitals were not allowed, although the MCSCF optimization of these orbitals was performed. The character of these states was easy to identify by analyzing the orbitals and CI expansion coefficients. The diagram in Figure 3

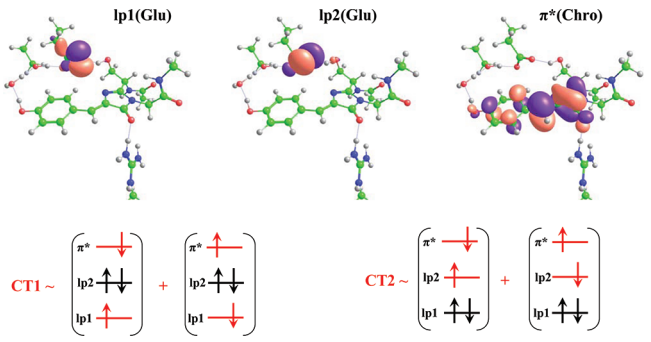

Figure 3. Top panel shows the key orbitals, namely, the lone-pair orbitals on Glu222 (lp1 and lp2) and the π^* orbital on Chro. Bottom panel illustrates the dominant electronic configurations contributing to the CT states S_{CT1} and S_{CT2}. The HOMO π orbital remains doubly occupied in the CT states.

illustrates the electronic structure of the two lowest CT states, S_{CT1} and S_{CT2}, computed by using the above protocol. Apparently, these two states are distinguished by electron transfers from different lone pair orbitals of Glu to the π^* orbital of Chro.

If we rely on the same model system as in the calculations of local Chro excitations (Table 2), i.e., the QM cluster shown by balls in sticks in Figure 1 and the same MCQDPT2/MCSCF quantum chemical approach, the $S_0 \rightarrow S_{CT1}$ and $S_0 \rightarrow S_{CT2}$ excitations (Table 4) are characterized by similar oscillator strengths (0.2 and 0.1). The computed excitation energies and the corresponding wavelengths are 4.0 (310) and 4.96 eV (250 nm). These values are consistent with the experimental values reported by van Thor et al.[16] (254 nm) and by Bell et al.[17] (254 and 280 nm) for the irradiation wavelengths initiating wt-GFP decarboxylation. We also report in the fifth row in Table 4 the excitation energies estimated for the QM cluster (Figure 1) in

Table 4. Excitation Energies (eV) of CT States S_{CTn} Calculated by Different Approaches[a]

model system, approximation	S_0-S_{CT1}	S_0-S_{CT2}
QM cluster (Figure 1) MCSCF/ORMAS/cc-pVDZ	4.10	5.14
QM cluster (Figure 1) MCQDPT2/MCSCF/ORMAS/cc-pVDZ	**4.0 (0.2)**	**4.96 (0.1)**
QM cluster (Figure 1) SOS-CIS(D)/cc-pVDZ	**4.70 (0.01)**	
QM cluster (Figure 1) + EFP, MCSCF/ORMAS/cc-pVDZ	5.32	6.04
QM cluster (Figure 1) + point charges, SOS-CIS(D)/cc-pVDZ	5.31 (0.03), 5.51 (0.06)	

[a]Oscillator strengths are given in parentheses.

the field of effective fragments; however, in this case we cannot compute directly perturbation energy corrections.

Reassuringly, we observe similar CT states in the SOS-CIS(D) calculations (Table 4), in which, of course, these states appeared as higher CI roots relative to the local Chro excitations. In the case of the QM cluster (Figure 1), we identified the only root of the CT character with the nonzero oscillator strength at 4.70 eV (264 nm) as reported in the fourth row in Table 4. Taking into account the point charges in the SOS-CIS(D) calculations resulted in two CT states with nonzero oscillator strengths (the last row in Table 4), in accord with the MCSCF/ORMAS calculations. Importantly, both theoretical approaches lead to a consistent conclusion: a couple of CT states may be directly accessible upon irradiation by the UV light source initiating decarboxylation. As discussed above, we rely on the estimates for the QM cluster shown in bold in Table 4; thus the energies of these states are between 4 and 5 eV (or between 250 and 310 nm). We remind that ref. 23 reports transition to the CT state at 4.18 eV (296 nm) with the oscillator of strength 0.027.

Effect of Thr203His Mutation. We investigated the effect of Thr203His mutation on the absorption spectra of GFP by using MCSCF without perturbation theory corrections. The primary goal was to estimate whether such mutation could affect energies of higher excited states presumably involved in the photoinduced decarboxylation. Therefore, we were not concerned in obtaining converged results for the absolute excitation energies. Using the molecular cluster shown in Figure 1 in the field of EFs, we computed the excitation energies for the locally excited states, S_1 and S_n, using the sa(10)-CASSCF(12/11)/6-31G* method, and the excitation energies to S_{CTn}, using MCSCF/ORMAS/6-31G*. Either Thr or His side chain at position 203 was included in the MM subsystem represented by EFs. The orientation of His was aligned manually following motifs of the crystal structure 3GJ1[20] followed by partial optimization. Table 5 lists the results of the calculations of excitation energies. We assumed that His is nonprotonated (neutral), which was consistent with the experimental observation[19] that the S_0-S_1 absorption band

Table 5. Excitation Energies (eV) for the Wild-Type and Thr203His Mutated GFP According to The QM/MM(EFP/AMBER) Estimates without Perturbation Corrections to the MCSCF Solutions

model system	S_0-S_1	S_0-S_x	S_0-S_{CT1}	S_0-S_{CT2}
wt-GFP	5.20	7.36	5.32	6.04
Thr203His variant	5.23	7.41	5.90	6.32

dx.doi.org/10.1021/ct300043e | J. Chem. Theory Comput. XXXX, XXX, XXX–XXX

maximum in the wild-type and the mutated protein was essentially the same.

We see that, in agreement with the experimental observations, this mutation has negligible effect on the S_0−S_1 excitation energy. However, the excitation energies of S_x and S_{CTn} are blue-shifted by 0.05 and 0.3−0.6 eV (i.e., up to 20 nm), respectively. Shifting S_x and S_{CTn} to higher energies increases the gap between the wavelength used to initiate the photoconversion and to excite fluorescence, which should reduce the read-out activation. We also note different magnitude of the shift for S_x and S_{CTn}. If the CT state can be blue-shifted even higher (or if S_x could be red-shifted), then the two-step route, $S_0 \rightarrow S_1 \rightarrow S_x$ will be shut down, which can be exploited in designing better photoconvertable FPs.

DISCUSSION

Our results suggest several possible scenarios for the primary photoconversion event in wt-GFP leading to population of a CT state which can be described as a Chro· and Glu222· biradical pair. Figure 4 presents relevant energy diagrams.

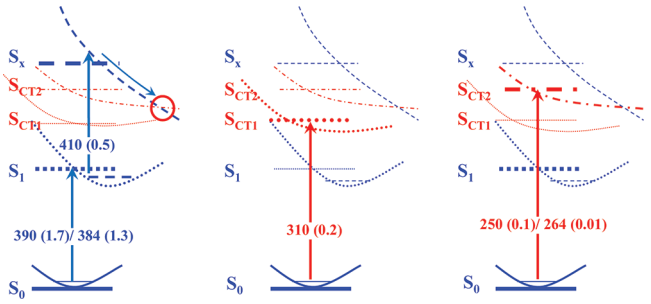

Figure 4. Energy diagrams illustrating electronic transitions leading to the CT states. The computed wavelengths (in nm) and corresponding oscillator strengths (in parentheses) are given in the order: the MCSCF-based values followed by the SOS-CIS(D) values when available.

As the left panel in Figure 4 illustrates, in the low-energy regime, the CT state can be accessed in a two-photon process via S_1. The computed oscillator strengths suggest one of the highly excited states S_X (here, S_7, counting the roots in our CASSCF procedure) as a likely target state that can then relax to one of the CT states via conical intersections, as indicated by the red circle in the left-side panel in Figure 4. The computed wavelengths of the sequential transitions $S_0 \rightarrow S_1 \rightarrow S_X$ (390/384 and 410 nm) are consistent with the light source of ∼400 nm used in the experiments of van Thor et al.[16a] and Brixner and co-workers.[18]

Alternatively, one can consider a two-step process in which the CT states are populated directly via S_1. To assess the feasibility of this scenario, we estimated oscillator strengths for the S_1−S_{CTn} transitions and found it to be around 0.02. Thus, the $S_0 \rightarrow S_1 \rightarrow S_{CTn}$ route cannot be excluded; however, the pathway via the locally excited state S_X, namely, $S_0 \rightarrow S_1 \rightarrow S_X \rightarrow S_{CTn}$, seems more probable because of more favorable oscillator strengths and better energy matching. However, in the experiments[18] using 800 nm (1.55 eV), in which decarboxylation is a three-photon process (1.55 × 3 = 4.65 eV), the energy of the CT states provides a better match (the S_X state is a little too high to be accessed at these conditions).

Although we did not compute the cross sections for the two-photon absorption (2PA), the oscillator strengths for one electron transitions ($S_0 \rightarrow S_1$, $S_1 \rightarrow S_X$, and $S_1 \rightarrow S_{CT1}$) show that the $S_0 \rightarrow S_X$ transition should have large 2PA cross sections due to the resonance enhancement. Such large resonance-enhanced 2PA cross sections in the UV region have been reported for several FPs.[49]

We suggest that the same mechanism ($S_0 \rightarrow S_1 \rightarrow S_X$) is operational in the experiments of Bell et al.[17] with even a lower-energy source 476 nm (2.6 eV). They noted that decarboxylation efficiency at this wavelength was marginally low. Because 476 nm corresponds to the S_0−S_1 excitation of the A-form of wt-GFP (i.e., containing the anionic chromophore), they suggested that in this low-energy regime the decarboxylation proceeds through the S_1 state of the anionic form and that electronically excited anionic chromophore acts as electron acceptor forming doubly charged negative anion. Such species are unstable in the gas phase and are likely to have relatively high energy even in the protein binding pocket. Moreover, the time-resloved study of Brixner and co-workers[18] argues in favor of initially excited neutral chromophore and not the fluorescent anionic intermediate to be a gateway state initiating decarboxylation. In summary, we consider direct involvement of the anionic form of the chromophore in the CT step to be unlikely.

We note that the reported threshold behavior[17] of decarboxylation in the low-energy regime (i.e., no photoconversion was observed with laser power below certain laser power threshold at 404 and 476 nm) is consistent with the two-photon process. Furthermore, the study of Brixner et al.[18] that quantified power dependence at low energies (400 and 800 nm) has shown, unambiguously, that decarboxylation is a two-photon process at 400 nm and a three-photon process at 800 nm.

In the high-energy (UV) regime, the CT states can be populated directly via one-photon excitation efficiently initiating the decarboxylation process, as illustrated in the right panels in Figure 4. The MCSCF-based calculations predict two CT states, at 310 and 250 nm. The SOS-CIS(D) calculations are in semiquantitative agreement with MCSCF and suggest that the CT states are strongly mixed with other excited states. The computed excitation energies of the CT band correlate with experimentally used wavelengths[16a,17] (280 and 254 nm).

CONCLUSIONS

Electronic structure calculations allow us to identify electronic states that are likely to be involved in the primary event of the decarboxylation process via a Kolbe mechanism. We propose the scenarios (summarized in Figure 4) of primary events in photoinduced decarboxylation of wt-GFP. In the high-energy UV regime, CT states, which can be described as Chro· and Glu222· biradical pair, can be populated directly via one-photon excitation efficiently initiating the decarboxylation process. In the low-energy regime, CT states can be accessed in a two- (or three-) photon process via S_1.

We also show that the point mutation Thr203His used, in particular, to construct PA-GFP, leads to blue-shifting energy levels of the S_{CTn} and S_X states by 0.3−0.6 eV (with the corresponding shifts in wavelengths up to 20 nm) and 0.05 eV, respectively, suggesting a possibility of a rational design of photoactivatable proteins in silico.

dx.doi.org/10.1021/ct300043e | J. Chem. Theory Comput. XXXX, XXX, XXX−XXX

■ ASSOCIATED CONTENT

Supporting Information

Details of the QM/MM model; the optimized coordinates of the QM subsystem; additional data (as compared to Table 1) on the CASSCF-based calculation results for the S_0-S_1 excitation energies; and figures of all active space orbitals from the CASSCF(12/11) and ORMAS calculations. This material is available free of charge via the Internet at http://pubs.acs.org.

■ AUTHOR INFORMATION

Corresponding Author

*E-mail: anemukhin@yahoo.com; anem@lcc.chem.msu.ru

Notes

The authors declare no competing financial interest.

■ ACKNOWLEDGMENTS

We thank Profs. A. P. Savitsky and V. V. Verkhusha for stimulating discussions. This work is partly supported by the Russian Foundation for Basic Research (project 10-03-0085) and by the Program of Molecular and Cell Biology from the Russian Academy of Sciences. We thank the Research Computing Center of M.V. Lomonosov Moscow State University and the Joint Supercomputer Center of Russian Academy of Sciences for providing computational resources. A.I.K. acknowledges the support from the National Science Foundation via the CHE-0951634 grant and from the Humboldt Foundation (Bessel Award).

■ REFERENCES

(1) Tsien, R. Y. *Annu. Rev. Biochem.* **1998**, *67*, 509−544.
(2) Zimmer, M. *Chem. Rev.* **2002**, *102*, 759−781.
(3) Wachter, R. M. *Photochem. Photobiol.* **2006**, *82*, 339−344.
(4) Meech, S. R. *Chem. Soc. Rev.* **2009**, *38*, 2922−2934.
(5) Day, R. N.; Davidson, M. W. *Chem. Soc. Rev.* **2009**, *38*, 2887−2921.
(6) van Thor, J. *J. Chem. Soc. Rev.* **2009**, *38*, 2935−2950.
(7) Chudakov, D. M.; Matz, M. V.; Lukyanov, S.; Lukyanov, K. A. *Physiol. Rev.* **2010**, *90*, 1103−1163.
(8) Wu, B.; Piatkevich, K. D.; Lionnet, T.; Singer, R. H.; Verkhusha, V. V. *Curr. Opin. Cell Biol.* **2011**, *23*, 310−317.
(9) Lukyanov, K. A.; Chudakov, D. M.; Lukyanov, S.; Verkhusha, V. V. *Nat. Rev. Mol. Cell Biol.* **2005**, *6*, 885−895.
(10) Lippincott-Schwartz, J.; Patterson, G. H. *Trends Cell Biol.* **2009**, *19*, 555−565.
(11) Dikici, E.; Daunert, S. *Nat. Chem. Biol.* **2009**, *5*, 70−71.
(12) Bogdanov, A. M.; Mishin, A. S.; Yampolsky, I. V.; Belousov, V. V.; Chudakov, D. M.; Subach, F. V.; Verkhusha, V. V.; Lukyanov, S.; Lukyanov, K. A. *Nat. Chem. Biol.* **2009**, *5*, 459−461.
(13) Subach, F. V.; Malashkevich, V. N.; Zencheck, W. D.; Xiao, H.; Filonov, G. S.; Almo, S. C.; Verkhusha, V. V. *Proc. Nat. Acad. Sci.U.S.A.* **2009**, *106*, 21097−21102.
(14) Subach, F. V.; Patterson, G. H.; Renz, M.; Lippincott-Schwartz, J.; Verkhusha, V. V. *J. Am. Chem. Soc.* **2010**, *132*, 6481−6491.
(15) Patterson, G. H. *J. Microsc.* **2011**, *243*, 1−7.
(16) (a) van Thor, J. J.; Gensch, T.; Hellingwerf, K. J.; Johnson, L. N. *Nat. Struct. Biol.* **2002**, *9*, 37−41. (b) van Thor, J. J.; Sage, J. T. *Photochem. Photobiol. Sci.* **2006**, *5*, 597−602.
(17) Bell, A. F.; Stoner-Ma, D.; Wachter, R. M.; Tonge, P. J. *J. Am. Chem. Soc.* **2003**, *125*, 6919−6926.
(18) Langhojer, F.; Dimler, F.; Jung, G.; Brixner, T. *Biophys. J.* **2009**, *96*, 2763−2770.
(19) Patterson, G. H.; Lippincott-Schwartz, J. *Science* **2002**, *297*, 1873−1877.
(20) Henderson, J. N.; Gepshtein, R.; Heenan, J. R.; Kallio, K.; Huppert, D.; Remington, S. J. *J. Am. Chem. Soc.* **2009**, *131*, 4176−4177.
(21) Laino, T.; Nifosì, R.; Tozzini, V. *Chem. Phys.* **2004**, *298*, 17−27.
(22) Das, A. K.; Hasegawa, J.-Y.; Miyahara, T.; Ehara, M.; Nakatsuji, H. *J. Comput. Chem.* **2003**, *24*, 1421−1431.
(23) Hasegawa, J.-Y.; Fujimoto, K.; Swerts, B.; Miyahara, T.; Nakatsuji, H. *J. Comput. Chem.* **2007**, *28*, 2443−2452.
(24) Bravaya, K. B.; Bochenkova, A. V.; Granovsky, A. A.; Nemukhin, A. V. *Russ. J. Phys. Chem. B* **2008**, *2*, 671−675.
(25) Topol, I.; Collins, J.; Polyakov, I.; Grigorenko, B.; Nemukhin, A. *Biophys. Chem.* **2009**, *145*, 1−6.
(26) Filippi, C.; Zaccheddu, M.; Buda, F. *J. Chem. Theory Comput.* **2009**, *5*, 2074−2087.
(27) Polyakov, I. V.; Grigorenko, B. L.; Epifanovsky, E. M.; Krylov, A. I.; Nemukhin, A. V. *J. Chem. Theory Comput.* **2010**, *6*, 2377−2387.
(28) Bravaya, K. B.; Grigorenko, B. L.; Nemukhin, A. V.; Krylov, A. I. *Acc. Chem. Res.* **2012**, *45*, 265−275.
(29) Filippi, C.; Buda, F.; Guidoni, L.; Sinicropi, A. *J. Chem. Theory Comput.* **2012**, *8*, 112−124.
(30) Sinicropi, A.; Andruniow, T.; Ferré, N.; Basosi, R.; Olivucci, M. *J. Am. Chem. Soc.* **2005**, *127*, 11534−11535.
(31) Bravaya, K. B.; Khrenova, M. G.; Grigorenko, B. L.; Nemukhin, A. V.; Krylov, A. I. *J. Phys. Chem. B* **2011**, *115*, 8296−8303.
(32) Creemers, T. M. H.; Lock, A. J.; Subramaniam, V.; Jovin, T. M.; Völker, S. *Nat. Struct. Biol.* **1999**, *6*, 557−560.
(33) Ormö, M.; Cubitt, A. B.; Kallio, K.; Gross, L. A.; Tsien, R. Y.; Remington, S. J. *Science* **1996**, *273*, 1392−1395.
(34) Grigorenko, B. L.; Nemukhin, A. V.; Topol, I. A.; Burt, S. K. *J. Phys. Chem. A* **2002**, *106*, 10663−10672.
(35) Nemukhin, A. V.; Grigorenko, B. L.; Topol, I. A.; Burt, S. K. *J. Comput. Chem.* **2003**, *24*, 1410−1420.
(36) Gordon, M. S.; Freitag, M. A.; Bandyopadhyay, P.; Jensen, J. H.; Kairys, V.; Stevens, W. *J. Phys. Chem. A* **2001**, *105*, 293−307.
(37) Yang, F.; Moss, L. G.; Phillips, G. N., Jr. *Nat. Biotechnol.* **1996**, *14*, 1246−1251.
(38) Ivanic, J. *J. Chem. Phys.* **2003**, *119*, 9364−9376.
(39) Nakano, H. *Chem. Phys.* **1993**, *99*, 7983−7992.
(40) Granovsky, A. A. *J. Chem. Phys.* **2011**, *134*, 214113.
(41) (a) Schmidt, M. W.; Baldridge, K. K.; Boatz, J. A.; Elbert, S. T.; Gordon, M. S.; Jensen, J. H.; Koseki, S.; Matsunaga, N.; Nguyen, K. A.; Su, S.; Windus, T. L.; Dupuis, M., Jr. *J. Comput. Chem.* **1993**, *14*, 1347−1363. (b) Gordon, M. S.; Schmidt, M. W. Advances in electronic structure theory: GAMESS a decade later. In *Theory and Applications of Computational Chemistry: the first forty years*; Dykstra, C. E., Frenking, G., Kim, K. S., Scuseria, G. E., Eds.; Elsevier: Amsterdam, The Netherlands, 2005; pp 1167−1189.
(42) Granovsky, A. A. *Firefly*, version 7.1.G; www http://classic.chem.msu.su/gran/firefly/index.html (accessed date December 29, 2011)
(43) Grimme, S. *J. Chem. Phys.* **2003**, *118*, 9095−9102.
(44) Rhee, Y. M.; Head-Gordon, M. *J. Phys. Chem. A* **2007**, *111*, 5314−5326.
(45) Krylov, A. I. *Annu. Rev. Phys. Chem.* **2008**, *59*, 433−462.
(46) Epifanovsky, E.; Polyakov, I.; Grigorenko, B.; Nemukhin, A.; Krylov, A. I. *J. Chem. Theory Comput.* **2009**, *5*, 1895−1906.
(47) Khrenova, M. G.; Nemukhin, A. V.; Grigorenko, B. L.; Krylov, A. I.; Domratcheva, T. M. *J. Chem. Theory Comput.* **2010**, *6*, 2293−2302.
(48) Shao, Y.; Molnar, L. F.; Jung, Y.; Kussmann, J.; Ochsenfeld, C.; Brown, S.; Gilbert, A. T. B.; Slipchenko, L. V.; Levchenko, S. V.; O'Neil, D. P.; Distasio, R. A., Jr.; Lochan, R. C.; Wang, T.; Beran, G. J. O.; Besley, N. A.; Herbert, J. M.; Lin, C. Y.; Van Voorhis, T.; Chien, S. H.; Sodt, A.; Steele, R. P.; Rassolov, V. A.; Maslen, P.; Korambath, P. P.; Adamson, R. D.; Austin, B.; Baker, J.; Bird, E. F. C.; Daschel, H.; Doerksen, R. J.; Drew, A.; Dunietz, B. D.; Dutoi, A. D.; Furlani, T. R.; Gwaltney, S. R.; Heyden, A.; Hirata, S.; Hsu, C.-P.; Kedziora, G. S.; Khalliulin, R. Z.; Klunziger, P.; Lee, A. M.; Liang, W. Z.; Lotan, I.; Nair, N.; Peters, B.; Proynov, E. I.; Pieniazek, P. A.; Rhee, Y. M.;

Ritchie, J.; Rosta, E.; Sherrill, C. D.; Simmonett, A. C.; Subotnik, J. E.; Woodcock, H. L., III; Zhang, W.; Bell, A. T.; Chakraborty, A. K.; Chipman, D. M.; Keil, F. J.; Warshel, A.; Herhe, W. J.; Schaefer, H. F., III; Kong, J.; Krylov, A. I.; Gill, P. M. W.; Head-Gordon, M. *Phys. Chem. Chem. Phys.* **2006**, *8*, 3172.
(49) Nifosì, R.; Luo, Y. *J. Phys. Chem. B.* **2007**, *111*, 14043−14050.